Journal of Orthopaedic Translation 24 (2020) 23–31

Contents lists available at ScienceDirect

Journal of Orthopaedic Translation

journal homepage: www.journals.elsevier.com/journal-of-orthopaedic-translation

Original Article

Changes of the end plate cartilage are associated with intervertebral disc degeneration: A quantitative magnetic resonance imaging study in rhesus monkeys and humans

Zemin Ling [a,1], Liangping Li [a,b,1], Yan Chen [a], Hao Hu [a], Xiaoxiao Zhao [c], Jordan Wilson [d], Qihua Qi [a], Delong Liu [a], Fuxin Wei [e], Xiaoying Chen [f], Jianhua Lu [g], Zhiyu Zhou [e], Xuenong Zou [a,*]

[a] Guangdong Provincial Key Laboratory of Orthopedics and Traumatology, Department of Spinal Surgery, The First Affiliated Hospital of Sun Yat-sen University, Guangzhou 510080, China
[b] Department of Orthopaedics, Sir Run Run Shaw Hospital, School of Medicine, Zhejiang University, Hangzhou, China
[c] Department of Radiology, The Eastern Hospital of the First Affiliated Hospital, Sun Yat-sen University, China
[d] Department of Orthopaedics, Johns Hopkins University School of Medicine, Baltimore, USA
[e] Department of Orthopaedic Surgery, The Seventh Affiliated Hospital and Orthopedic Research, Institute of Sun Yat-sen University, Shenzhen, China
[f] Department of Emergency, The Second Affiliated Hospital of Zhejiang University School of Medicine, Hangzhou, 310009, China
[g] Department of Radiology, Johns Hopkins Hospital, Baltimore, USA

ARTICLE INFO

Keywords:
End plate
Intervertebral disc degeneration
MRI
T2 map
Rhesus monkeys

SUMMARY

Background: The end plate plays an important role in intervertebral disc degeneration progression. The aim of the study was to examine the compositional and structural changes of the end plate with age and to investigate the correlation between end plate and disc degeneration by T1ρ and T2 map magnetic resonance imaging.

Methods: There were 12 young monkeys (6-7 years old), 20 aged monkeys (14-17 years old) and 12 human participants (30-50 years old) in this study. T1ρ or T2 map values of the nucleus pulposus and end plate cartilage were analyzed according to Pfirrmann grades and age. Afterwards, micro computed tomography and histological analysis were used to confirm the end plate changes in monkeys. Pearson's correlation was performed to investigate the relationship between end plate and disc degeneration.

Results: In monkeys, T1ρ (r=-0.794, $P<0.001$) and T2 map values (r=-0.8, $P<0.001$) of the nucleus pulposus were negatively associated with Pfirrmann grades. Moreover, the T2 map was more suitable than T1ρ for the evaluation of end plate degeneration. Age was an important influence factor of end plate and disc degeneration, which was confirmed by microcomputed tomography, Safranin O/fast green staining, and collagen II staining. The T2 map value of lower end plate degeneration positively correlated with that of the intervertebral discs in monkeys (R^2=0.3133, $P<0.001$) and humans (R^2=0.2092, $P<0.001$).

Conclusion: This study suggests that the compositional and structural changes of the end plate can be quantitatively evaluated by T2 map. Furthermore, cartilage end plate degeneration is associated with disc degeneration during ageing.

The translational potential of this article: A better understanding of how the cartilage end plate affects disc degeneration is needed, which may propose a new clinical application using T2 map to evaluate end plate degeneration.

* Corresponding author.
E-mail addresses: lingzm@mail2.sysu.edu.cn (Z. Ling), lliangp2018@zju.edu.cn (L. Li), coboyoung@gmail.com (Y. Chen), huhaosysu@hotmail.com (H. Hu), 1186159543@qq.com (X. Zhao), Jordanpwpw@gmail.com (J. Wilson), qqhua1938@126.com (Q. Qi), 651464711@qq.com (D. Liu), suifeng720@163.com (F. Wei), 2515169@zju.edu.cn (X. Chen), lujianhua01@gmail.com (J. Lu), zzy990802@126.com (Z. Zhou), zxnong@hotmail.com (X. Zou).
[1] These authors contributed equally to this work.

https://doi.org/10.1016/j.jot.2020.04.004
Received 20 November 2019; Received in revised form 10 March 2020; Accepted 9 April 2020
Available online 8 May 2020

Introduction

Low back pain (LBP) is a common clinical and public health problem. An estimated 149 million workdays are lost every year in the United States because of LBP [1], with total costs estimated to be $100–200 billion annually [2]. Substantial evidence links LBP to lumbar intervertebral disc degeneration (IDD) [3,4]. The aetiology of IDD is multifactorial, and there are various aetiological factors including genetics [5], gender [6], ageing [7], smoking [8], high mechanical stress [9], and insufficient nutrition [10]. However, a clear understanding of the pathogenesis of IDD is limited.

The cartilage end plate is connected to the vertebral bone and disc, and the degeneration or sclerosis of the end plate may induce metabolic disorder in the disc [11,12]. Cartilaginous end plates resist intervertebral pressure and allow nutrient diffusion into the avascular disc from vertebral blood vessels [13,14]. The end plate becomes sclerotic and less permeable with age, resulting in reduced nutrient transport to the nucleus pulposus (NP) [15,16]. Our prior work has shown that nutrition disorder is a key factor leading to IDD by sub–end plate injection of pingyangmycin to produce a "devascular effect" in rhesus monkeys, which created a disease model mimicking the onset of disc degeneration in humans [17]. Although nutrition disorder has been proposed to be a common pathway of IDD [18], the role of end plate degeneration in the progression of disc degeneration remains largely unknown.

Magnetic resonance imaging (MRI) is the most effective imaging modality in the diagnosis of IDD. With disc degeneration, a reduction in signal intensity on T2-weighted images is observed in the NP, with eventual loss of distinction between the NP and annulus fibrosus [19]. Some newly developed quantitative MRI techniques, such as T1ρ and T2 map, can provide information about biochemical composition and structural integrity of degenerated discs in a noninvasive manner [20]. T1ρ relaxation time (T1ρ values) is predominantly influenced by proteoglycan [21–23], while T2 map relaxation time (T2 map values) depends on collagen anisotropy and water content [30]. Our previous study has also demonstrated that T1ρ values of the NP were inversely correlated with Pfirrmann grades in both humans and rhesus monkeys and suggested that T1ρ MRI technique is potentially a precise and noninvasive tool to detect changes of biochemical composition in lumbar IDD.

Despite the potentially important role of the end plate in disc degeneration, the relationship between the end plate and disc degeneration with age has not been well clarified. In addition, disc degeneration is often assessed using the Pfirrmann grading system, which is only a semiquantitative method [25]. This study aimed to determine whether end plate degeneration can be quantitatively evaluated by T1ρ or T2 map and to investigate its relationship with disc degeneration. To this aim, we focused on the end plate and disc degeneration in rhesus monkeys and humans and investigated their correlations using T1ρ or T2 map MRI in an attempt to understand the natural history and the changes of the end plate in the degeneration of the intervertebral disc, which may uncover the function of the end plate in disc degeneration.

Materials and methods

The study protocol was reviewed and approved by the Institutional Review Board and Ethics Committee of the First Affiliated Hospital of Sun Yat-sen University in Guangzhou, China (no. 2010-094 and no. 2018-053). The animal study was approved by the Institutional Review Board and Animal Care Committee of the First Affiliated Hospital of Sun Yat-sen University (SYXK-2016-0112) and Guangdong Institute of Biological Resources, Guangzhou, China (SYXK-2018-0187).

Human participants

From June 2016 to May 2017, 12 of the outpatients (5 women and 7 men; median age: 43 years) with LBP, who consulted with Xu.Z. in the orthopaedic clinic at the First Affiliated Hospital of Sun Yat-sen University, participated in this study. The inclusion criteria specified that participants must be actively working, be between ages 30 and 50 years, and have only experienced a single episode of LBP. Exclusion criteria was as follows: body mass index higher than 35, radicular pain, neurologic deficits of the lower limbs, previous spine surgery, contraindications for MRI, known intervertebral disk herniation within the past two years, or known lumbar scoliosis of more than 15° in coronal MRI.

Rhesus monkeys

Thirty-two rhesus monkeys were used for MRI scanning in this study. There were 12 young monkeys (6 males and 6 females; median age: 7 years; range: 6–7 years) and 20 aged monkeys (13 males and 7 females; median age: 16 years; range: 14–17 years [26]). One young and one aged monkey were sacrificed for histological analysis after MRI scanning.

MRI acquisition

All MRI examinations were performed on human participants and rhesus monkeys lying in the supine position using a 1.5-T MR scanner (Philips Achieva, Amsterdam, Netherlands). The monkeys were under anaesthesia. The imaging protocol for both humans and animals included multiple sections of two-dimensional sagittal and axial T1- and T2-weighted fast spin-echo sequences and quantitative MRI acquired with T1ρ and T2 quantification sequences (Table 1) previously developed in our laboratory [27]. MRI of the lumbar spine (L1–S1) in monkeys was performed.

Region of interest quantification and Pfirrmann grading

T1ρ values were calculated using Siswin software (version 0.9; Siswin, MR Research Centre at Aarhus University Hospital, Denmark). T2

Table 1
Parameters for MRI of rhesus monkeys and humans.

Parameter	T1-weighted	T2-weighted	T1 ρ*	T2 map
Pulse sequence	TSE	TSE	TSE	TSE
Monkey				
Repetition time (ms)	400	2500	800	2000
Echo time (ms)	7.8	100	8	TE**
Field of view (mm)	210 × 210	210 × 210	210 × 210	210 × 210
Pixel bandwidth (Hz)	242	475	332	234
Voxel size (mm)	0.9 × 1.25	0.9 × 1.25	0.59 × 1.17	0.7 × 0.8
Section thickness (mm)	3	3	3	3
Section gap (mm)	0	0	0	0
Number of sections	7	7	4 × 7	8 × 7
Turbo factor	4	45	12	8
Acquisition time (ms)	140	80	451	526
Human				
Repetition time (ms)	448	3228	800	2000
Echo time (ms)	8	100	8	TE**
Field of view (mm)	250 × 250	250 × 250	240 × 240	240 × 240
Pixel bandwidth (Hz)	320	348	348	234
Voxel size (mm)	0.9 × 1.25	0.9 × 1.25	0.59 × 1.17	0.7 × 0.8
Section thickness (mm)	3	3	3	3
Section gap (mm)	0	0	0	0
Number of sections	15	15	4 × 16	8 × 16
Turbo factor	4	45	12	8
Acquisition time	208	160	260	526

*Time of spin locking at 2, 15, 30, and 45 ms.
**Time of spin locking at 11, 22, 32, 43, 54, 65, 76, and 85 ms.
MRI = magnetic resonance imaging; TSE = turbo spin echo; TE = the echo time.

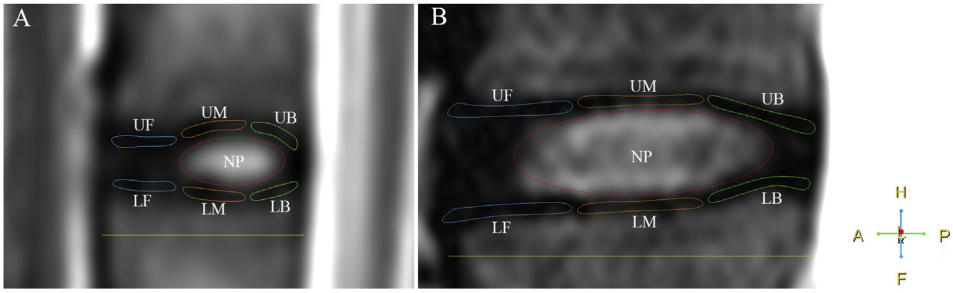

Figure 1. (A) Measuring T1ρ and T2 map values of the region of interest of the nucleus pulposus in the end plate and the lumbar intervertebral disc of rhesus monkeys. (B) Measuring T1ρ and T2 map values of the region of interest of the nucleus pulposus in the end plate and the lumbar intervertebral disc of humans. The regions of interest are shown in the T2 weighted image. A = anterior; F = feet; H = head; LB = lower back; LF = lower front; LM = lower middle; NP = nucleus pulposus; P = posterior; UB = upper back; UF = upper front; UM = upper middle.

map values were calculated using Siswin software or Philips DICOM viewer (R3.0-SP12, Philips Healthcare, Amsterdam, Netherlands). The regions of interest (ROIs) were chosen in the centre of the NP (1 cm^2 on images of humans, 0.1 cm^2 on images of monkeys) and the front, middle and back, upper, or lower third of the end plate (20 mm^2 on images of humans, 4 mm^2 on images of monkeys), as shown in Fig. 1. Three radiologists who were blinded to the study groups measured the values of the ROIs and graded all intervertebral discs using the T2-weighted images as per the classification scale of Pfirrmann, as described in a previous report [25,27].

Microcomputed tomography

One young and one aged monkey were euthanized after MRI scanning

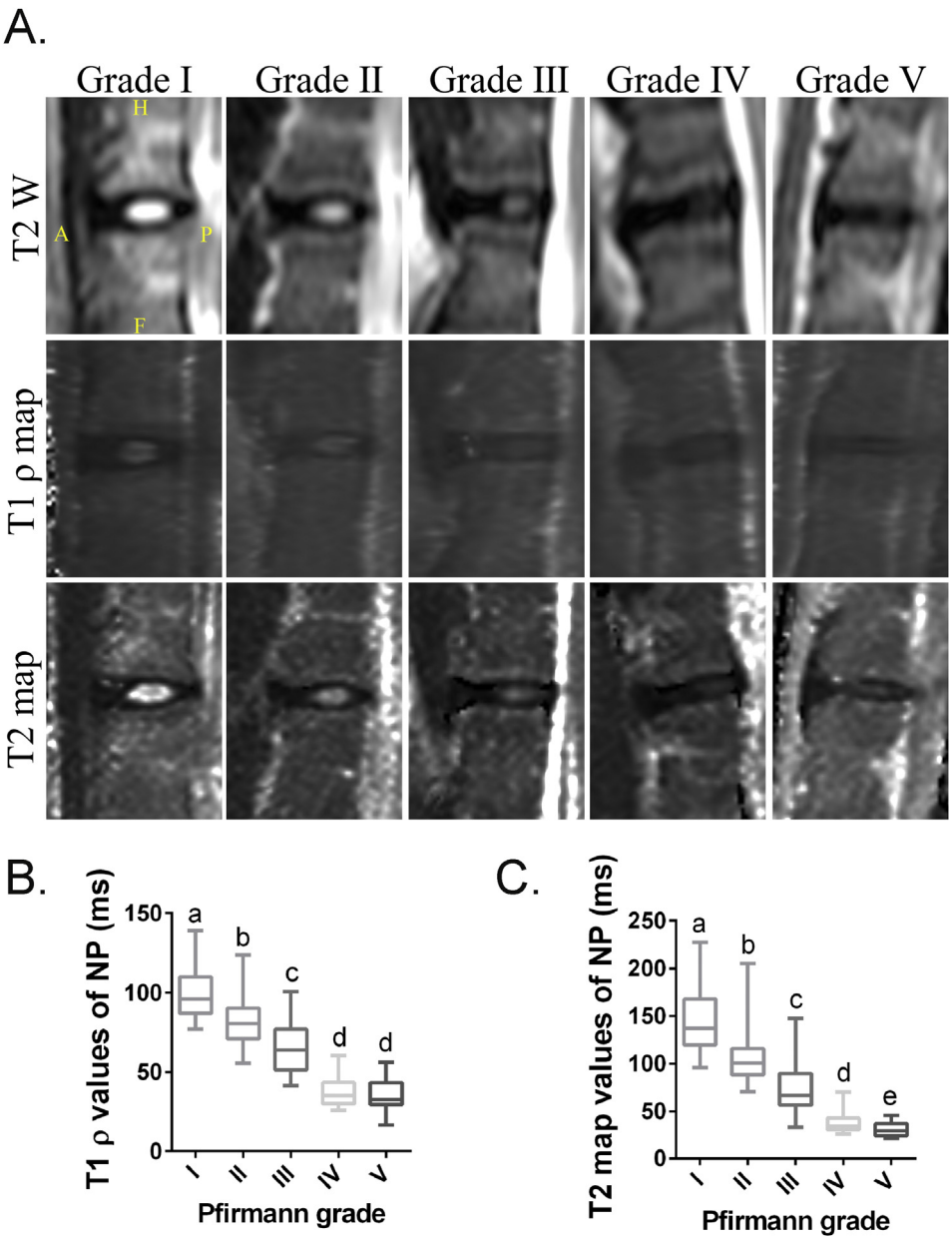

Figure 2. (A) T2-weighted, T1ρ, and T2 map images of lumbar intervertebral discs (IDD) related to Pfirrmann grades in rhesus monkeys. (B) The box plot graph (median and interquartile range) shows Pfirrmann grade of rhesus monkeys lumbar IDD and its corresponding T1ρ values. (C) The box plot graph (median and interquartile range) shows Pfirrmann grade of rhesus monkeys lumbar IDD and its corresponding T2 map values. Bars with different superscript letters (a, b, c, d, e) are significantly different at $P < 0.05$. A = anterior; F = feet; H = head; IDD = intervertebral disc degeneration; NP = nucleus pulposus; P = posterior.

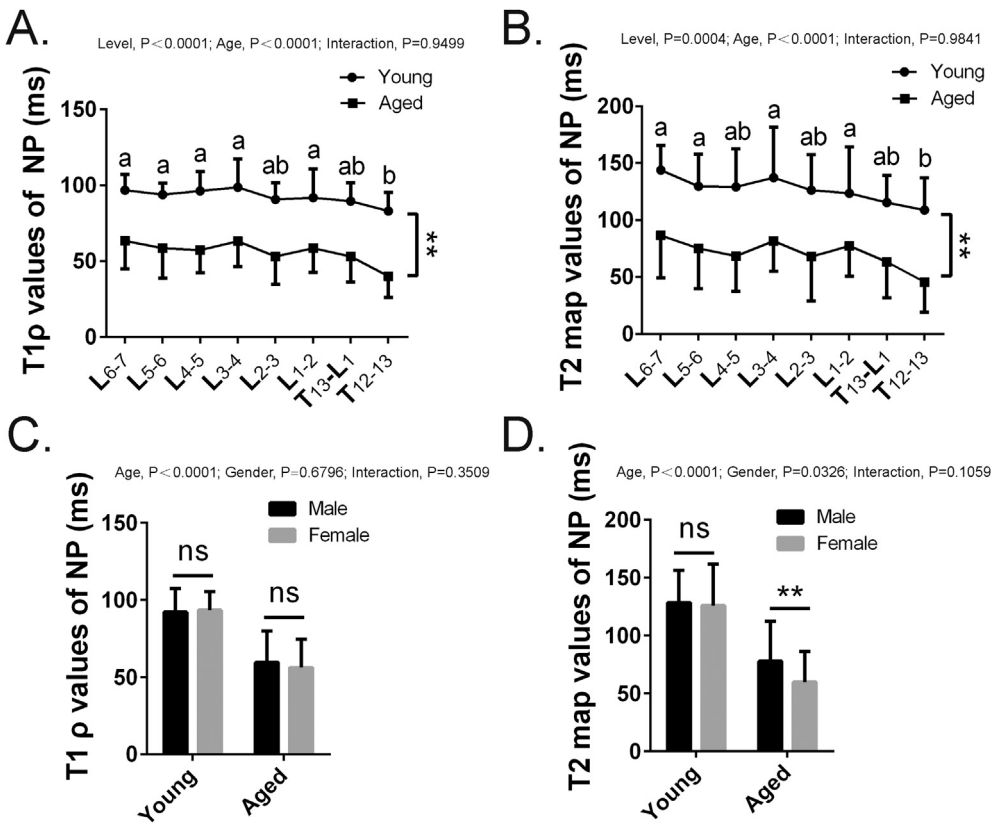

Figure 3. (A and B) T1 ρ and T2 map values of the nucleus pulposus of the intervertebral disc by different segments of young and aged rhesus monkeys. (C and D) T1 ρ and T2 map values of the nucleus pulposus of the intervertebral disc by gender of young and aged rhesus monkeys. Data are shown as mean ± SD. Bars with different superscript letters (a, b) are significantly different at $P < 0.05$. *p <0.05; **p <0.01. SD = standard deviation.

and flushed with phosphate-buffered saline for 10 min, followed by 10% buffered formalin perfusion for 5 min. The lower thoracic and whole lumbar spine were dissected and fixed in 10% buffered formalin for 48 h. High-resolution microcomputed tomography (μCT) (Skyscan1172, Bruker, Kontich, Belgium) was used to examine end plate changes. The scanner was set at a voltage of 55 kVp, a current of 181 μA, and a resolution of 12.0 μm per pixel. Images were reconstructed and analyzed using NRecon version 1.6 and CTAn version 1.9 (Skyscan company, San Jose, CA, USA), respectively.

Histomorphometry and immunohistochemistry

After μCT, the spine samples (T13–L7) were transferred to 0.5 M EDTA (pH 7.4) for complete decalcification and then embedded in paraffin. Four-micrometre-thick, sagittal-oriented sections of the spine were processed for Safranin O and fast green staining and immunohistochemistry staining by using a standard protocol. The sections were incubated with primary antibodies to rabbit type II collagen (1:100, ab34712; Abcam, Cambridge, UK) or Bovine Serum Albumin (BSA, 1%, negative control) overnight at 4 °C. Then, the corresponding secondary antibodies were added onto the sections for 1 h, followed by the use a horseradish peroxidase–streptavidin detection system (Dako, Agilent, Santa Clara, USA) to detect immunoactivity. Slides were then counterstained with haematoxylin (Sigma-Aldrich, St. Louis, USA). ImageJ (National Institutes of Health, Bethesda, USA) software was used for quantitative analysis, including the thickness and type II collagen–-positive area of the end plate.

Statistical analysis

Statistical analysis was performed using SPSS 23.0 software (SPSS, Chicago, USA). One-way analysis of variance (ANOVA) and multiple comparisons were used to compare three or more groups of T1ρ or T2 map values of the end plate or the NP by Pfirrmann grades. Two-way ANOVA was used to analyze T1ρ or T2 map values of the NP to evaluate the effect of age, gender, and spinal level in degenerated discs. The difference between the young and aged groups of T1ρ or T2 map values of the end plate or the NP was probed using the Student t test. Pearson's correlation analysis was performed to investigate the relationship between the end plate and the NP in the T1ρ or T2 map values for both the humans and the monkeys. Spearman's rank correlation was used to investigate the relationship between the Pfirrmann classification system and the T1ρ or T2 map values for monkeys. The difference of the thickness and type II collagen–positive area in the end plate of two groups was analyzed using the Student t test. A difference between groups was considered statistically significant if the *P* value was less than 0.05.

Results

T1ρ and T2 map values of the NP were negatively correlated with Pfirrmann grades in rhesus monkeys

A total of 256 intervertebral discs from rhesus monkeys were scanned and evaluated based on typical MRI scans, including T2-weighted images, T1ρ values, and T2 maps (Fig. 2A). These discs were classified into Grade I (n = 37), Grade II (n = 115), Grade III (n = 35), Grade IV (n = 35), and Grade V (n = 34) as per the Pfirrmann grading system.

As our previous study in humans, T1ρ values were also significantly correlated with Pfirrmann grades in rhesus monkeys ($r = -0.794$, $P < 0.0001$). The mean and standard deviation of T1ρ values of the NP by Pfirrmann grades were as follows: 98.47 ± 14.25 (grade I), 81.92 ± 14.38 (grade II), 64.62 ± 14.51 (grade III), 37.37 ± 8.80 (grade IV), and 35.60 ± 9.07 (grade V) (Fig. 2B). Moreover, the T2 map values of the NP were also significantly associated with Pfirrmann grades

($r = -0.8$, $P < 0.0001$). The mean T2 map values by Pfirrmann grades were as follows: 143.7 ± 31.51 (grade I), 105.8 ± 27.17 (grade II), 74.57 ± 26.39 (grade III), 36.88 ± 9.90 (grade IV), and 30.95 ± 7.249 (grade V) (Fig. 2C).

There were also significant differences between Pfirrmann Grades I–IV in both T1ρ and T2 map values of the NP ($P < 0.0001$). However, there were significant differences between Pfirrmann Grade IV and Grade V only in T2 map values ($P = 0.045$), but not in T1ρ values ($P = 0.49$) (Fig. 2B and C). This indicated that T2 map is more sensitive than T1ρ for identifying the differences between the two most advanced Pfirrmann grades (IV and V). Collectively, these findings suggested that both T1ρ and T2 map were good ways to quantitatively evaluate the degeneration of the NP in rhesus monkeys, but T2 map may be more sensitive in the late stage of IDD than T1ρ.

Age is an important aetiological factor of disc degeneration in rhesus monkeys

To examine if disc degeneration was accompanied by age, we calculated T1ρ and T2 map values of the disc segments in aged and young rhesus monkeys from T12 to L7. We then analyzed the relationship between age and spinal levels in disc degeneration using two-way ANOVA. The results showed that both age ($P < 0.0001$) and spinal level ($P < 0.0001$) were the main effects. The T1ρ values (Fig. 3A) and T2 map values (Fig. 3B) of the NP were significantly higher in all segments of the young group than in those of the aged group (both $P < 0.0001$), indicating the development of disc degeneration with age. For T1ρ values, the values of T12–T13 discs were significantly lower than those of the other segments, but not L2–3 or T13–L1. The same trend was also found in T2 map values, which indicated that the thoracolumbar segments were more susceptible to degeneration with age in monkeys. Next, we measured the T1ρ and T2 map values between male and female groups. For T1ρ values, there was no significant difference in gender ($P = 0.6796$) or the interaction between age and gender ($P = 0.3509$) (Fig. 3C). However, the significant differences in gender were found in T2 map values ($P = 0.0326$) (Fig. 3D), which indicated that females may be more vulnerable to disc degeneration during ageing than males. Furthermore, the results also suggested that T2 map might be superior to T1ρ in the assessment of the middle and late stage of IDD.

End plate degeneration with age can be quantitatively and precisely evaluated by T2 map

The ROIs of end plates were analyzed and are shown in Fig. 1. In comparison with the young group, the T1ρ values of the whole end plate significantly decreased in the aged group (Table 2). Moreover, after comparing T1ρ values of the end plates among the three groups (mild, >80 ms; moderate, 40–80 ms; severe, 10–40 ms) based on T1ρ values of the NP, only the upper and lower back end plates had significant differences (Table 2, left). In addition, T2 map values of the upper middle and lower front, middle, and back end plates in the aged group were lower than those of the young group. This indicates that there are differences in age-related dehydration and sclerosis among different parts of the end plate. Interestingly, comparing T2 map values among the three groups (mild, >100 ms; moderate, 40–100 ms; severe, 10–40 ms) based on T2 map values of the NP, significant differences were also found in the same sites of the end plate (Table 2, right). Taken together, these findings suggested that end plate degeneration can be quantitatively evaluated by T1ρ and T2 map, but it may be more precisely evaluated by T2 map.

Compositional and structural changes of the end plate with age

Site-matched μCT and histologic examinations were used to confirm compositional and structural changes of the end plate in young and aged monkeys. μCT showed that the end plate became more sclerotic in the segments with low T2 map values of the NP (Fig. 4A). Similar results

Table 2
T1ρ and T2 map values of ROIs in young and aged rhesus monkeys.

The regions of interest	T1ρ value						T2 map value						
	Ageing (n = 160)	Young (n = 96)	*P*	Severe (10–40 ms), (n = 36)	Moderate (40–80 ms), (n = 118)	Mild (>80 ms), (n = 102)	*P*	Ageing (n = 160)	Young (n = 96)	*P*	Severe (10–40 ms), (n = 33)	Moderate (40–100 ms), (n = 125)	Mild (>100 ms), (n = 98)	*P*
Nucleus pulposus	58.77 ± 19.95	92.81 ± 13.69	<0.0001	31.64 ± 4.81	62.75 ± 12.13	94.72 ± 12.10	<0.0001	72.02 ± 33.02	126.91 ± 32.59	<0.0001	29.93 ± 4.59	75.64 ± 17.91	130.50 ± 28.92	<0.0001
End plate upper front	29.61 ± 9.46	32.30 ± 7.81	0.020	28.94 ± 10.14	30.04 ± 8.60	31.79 ± 8.93	0.176	26.48 ± 8.98	27.47 ± 8.71	0.389	24.58 ± 7.52	27.00 ± 8.89	27.44 ± 8.18	0.237
Upper middle	29.99 ± 9.42	32.63 ± 7.61	0.021	30.61 ± 11.34	30.54 ± 8.66	31.50 ± 7.87	0.705	31.71 ± 9.96	34.60 ± 10.65	0.030	27.12 ± 5.04	31.88 ± 8.46	35.61 ± 10.24	<0.0001
Upper back	33.76 ± 9.06	35.62 ± 8.71	0.107	31.36 ± 10.31	34.16 ± 7.87	35.82 ± 9.47	0.034	30.36 ± 9.18	31.30 ± 7.42	0.400	30.64 ± 6.70	30.00 ± 8.41	31.47 ± 9.48	0.455
Lower front	29.32 ± 7.70	31.90 ± 6.80	0.007	29.63 ± 8.21	29.29 ± 7.11	31.62 ± 7.50	0.058	25.18 ± 8.09	27.87 ± 6.07	0.005	22.67 ± 7.33	25.76 ± 7.02	27.78 ± 6.78	0.001
Lower middle	31.24 ± 9.17	33.53 ± 7.49	0.039	31.24 ± 9.39	30.98 ± 9.05	33.67 ± 7.64	0.055	33.09 ± 8.48	40.34 ± 9.01	<0.0001	29.73 ± 6.66	32.67 ± 6.94	41.01 ± 9.65	<0.0001
Lower back	34.82 ± 8.34	37.12 ± 8.55	0.034	31.75 ± 10.20	35.41 ± 6.95	37.27 ± 9.09	0.003	30.18 ± 5.96	33.29 ± 6.39	0.0001	28.89 ± 6.09	30.34 ± 5.68	33.18 ± 6.28	0.0001

ROIs = regions of interest.

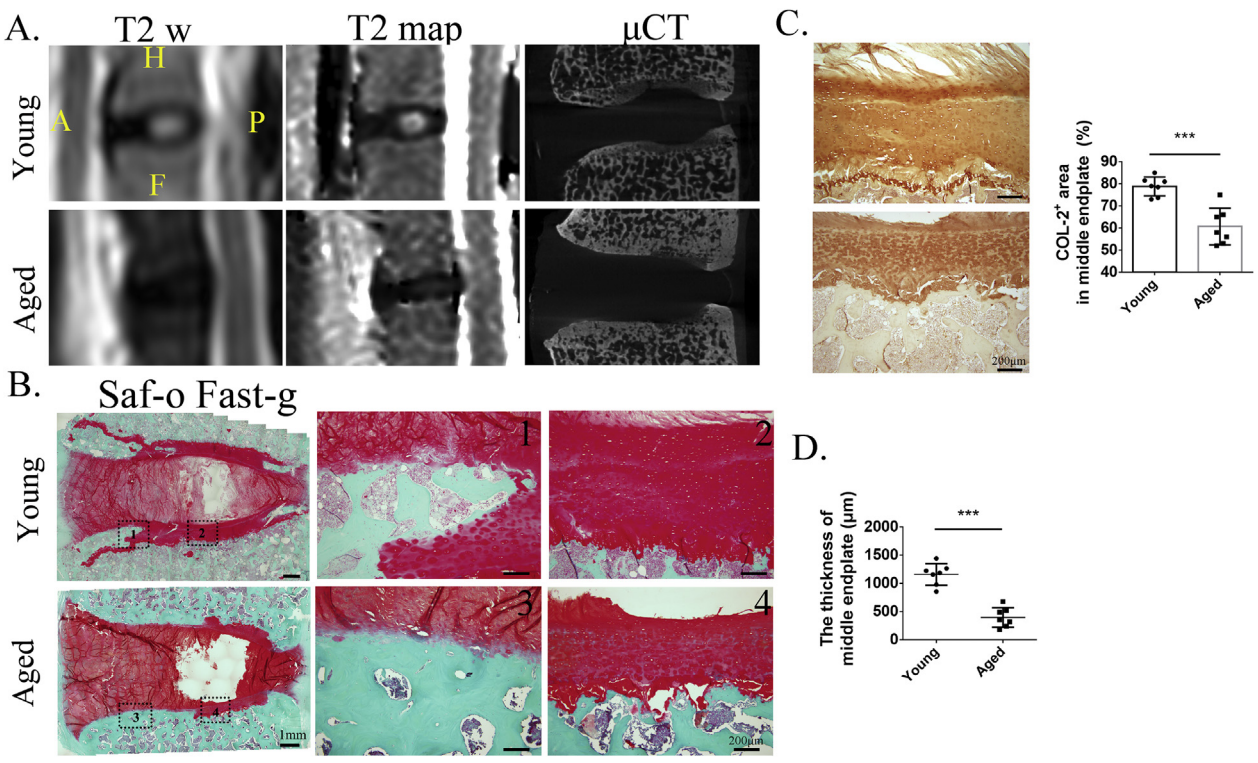

Figure 4. (A) End plate changes including μCT and Safranin O and fast green staining in the young and aged monkeys with high or low T2 map values of the intervertebral disc. (B) The sclerotic end plate occurred in the front one-third of the end plate (1 and 3); the cartilage in the middle one-third of the end plate of the aged group (4) was thinner than that in the young group (2). (C) And the immunohistology staining of type II collagen showed that type II collagen–positive area (brown) was lower expression in the aged group than that in the young group. (D) The thickness of middle end plate had been calculated, and there were statistically significant differences in the two groups. μCT = microcomputed tomography.

were also observed with Safranin O/fast green staining (Fig. 4B). Interestingly, the lower front and middle end plates also became sclerotic, where a lot of cartilage was replaced with new bone formation, not only in the aged but also in the young group. The cartilage of the middle end plate in the aged group was significantly thinner than that in the young group (Fig. 4B and D). Immunostaining also showed less type II collagen in the middle end plate in the aged monkeys (Fig. 4C) but that in the negative control was blank (data not shown in the figure). Given these findings, these data confirmed that the compositional and structural changes of the end plate with age were reflected by T2 map values, again suggesting that end plate degeneration can be precisely evaluated by T2 map.

Positive correlations between T2 map values of the end plate and NP in rhesus monkeys

Linear regression between the T2 map values of the end plate and the NP (Fig. 5) showed that the whole lower end plate ($R^2 = 0.3133$, $P < 0.0001$), especially the lower middle ($R^2 = 0.2845$, $P < 0.0001$), had a significant positive correlation with the NP. Although there were

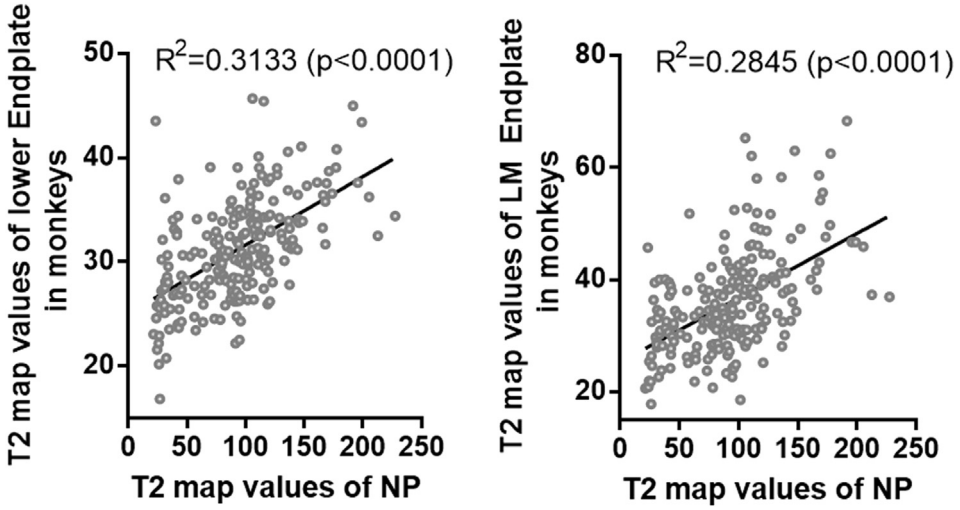

Figure 5. Correlation between the T2 map values of the nucleus pulposus (NP) and the lower end plate or lower middle (LM) end plate in rhesus monkeys had been analyzed. The T2 map values of the NP and the T2 map values of the lower end plate or lower middle end plate were significantly positively correlated.

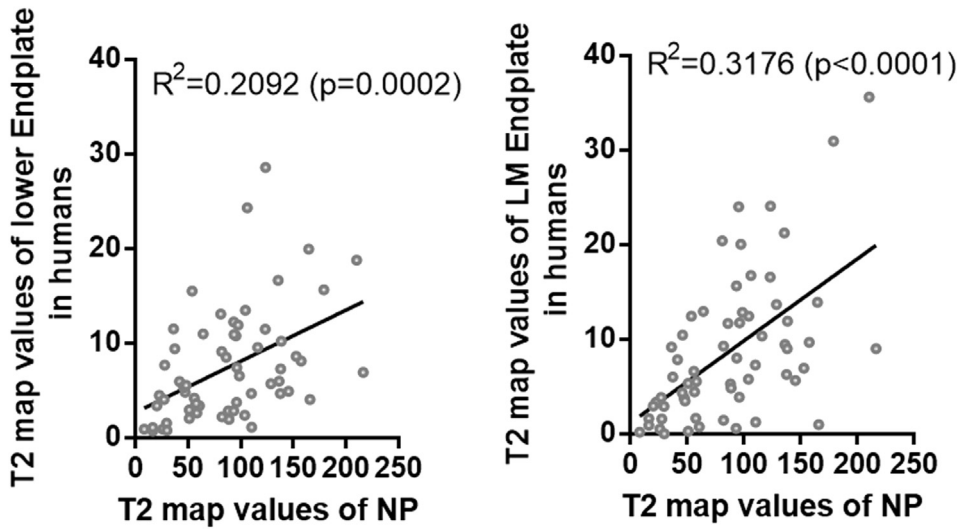

Figure 6. Correlation between the T2 map values of the nucleus pulposus (NP) and the lower end plate or lower middle (LM) end plate of 12 outpatients had been analyzed. There was significant positive correlation between the T2 map values of the NP and the T2 map values of the lower end plate, especially between the lower middle end plate and the NP.

significant correlations between T2 map values of other ROIs and the NP, the correlation coefficients were lower than 0.3. The exceptions were the whole upper ($r = 0.33$, $P < 0.0001$) and upper middle end plate ($r = 0.38$, $P < 0.0001$), but they were lower than 0.5 (Supplementary Table 1A). Thus, these data suggested lower end plate degeneration was associated with disc degeneration in rhesus monkeys, especially in the lower middle end plate.

Positive correlations between T2 map values of the end plate and the NP in humans

At the same time, MRI and analysis of T1ρ and T2 maps were also performed in voluntary outpatients (Supplementary Table 1B). Even with limited human participants, linear regression between the T2 map values of the end plate and the NP showed that average T2 map values of the lower whole end plate ($R^2 = 0.2092$, $P = 0.0002$), especially the lower middle end plate ($R^2 = 0.3176$, $P < 0.0001$), had a significant positive correlation with those of the NP (Fig. 6), which confirmed the results of rhesus monkeys.

Discussion

To the best of our knowledge, this study is the first investigation of end plate degeneration and its relationship with IDD in nonhuman primates using quantitative MRI. In the present study, we found that T1ρ and T2 map values of the NP had significant negative correlations with Pfirrmann grades in the disc of rhesus monkeys. Moreover, the end plate structure could be easily distinguished with the T1ρ and T2 map image. End plate degeneration can be quantified by T1ρ and T2 map, while T2 map may be more sensitive to mid- to late-stage changes. Furthermore, regression analysis demonstrated that T2 map values of the end plate, especially in the lower middle region, were closely associated with T2 map values of the NP, which had lower thickness and type II collagen in the aged group, as shown by histologic examination. What is more, the data from human participants confirmed the correlation, suggesting that lower middle end plate degeneration is highly associated with disc degeneration in both aged rhesus monkeys and humans.

Early biochemical changes of IDD include a decrease in proteoglycan levels and hydration [28]. Morphological changes including NP dehydration, collagen disarrangement, end plate sclerosis, and disc height loss occur in advanced IDD. The findings from Johannessen et al. [29] indicated that T1ρ was correlated with sulphated glycosaminoglycan content in the human NP. Our previous study has demonstrated that there was a significant negative correlation between T1ρ values of the NP and Pfirrmann grades in humans and rhesus monkeys [27]. Decreased T2 map values were caused by collagen disarrangement and hydration in the intervertebral disc [30]. In the present study, we found that both T1ρ and T2 map values of the NP had significant inverse correlations with Pfirrmann grades in rhesus monkeys. Moreover, T2 map can distinguish the differences between Pfirrmann Grades IV and V in the female and male group of aged monkeys, which indicates that T2 map might be more sensitive for evaluating and quantifying the middle and late stage of IDD.

End plate degeneration on MRI was first described by Modic et al. [47] and classified into three types according to the signal changes of the bone marrow. T1ρ and T2 map were mainly used to evaluate cartilage degeneration in osteoarthritis or disc degeneration in orthopaedic research, although they were also used to evaluate bone quality by reflecting the water content in cortical bone [31–33], and bone marrow oedema-like lesions [34,35]. In our study, end plate degeneration was quantified and manifested by reduced values of T1ρ and T2 map, which reflected biochemical composition and structural changes of the end plate with age. Moreover, these compositional and structural changes of the end plate cartilage during ageing can be precisely evaluated by T2 map in young and aged monkeys, which were confirmed by site-matched μCT and histological examination. Furthermore, we found that there was a close correlation between the T2 map value of the end plate, especially the lower middle region, and NP degeneration in rhesus monkeys. This observation was also confirmed by data from human participants.

The avascular disc depends on diffusion and convection through the end plate cartilage for nutrient supply and metabolite removal. With degeneration, the end plate becomes sclerotic and less permeable, and consequently, nutrient transport to the NP across the end plate reduces [12]. Given the results of the present study, our data suggest that insufficient nutrition caused by compositional and structural changes of the lower middle end plate during ageing is an important aetiological factor leading to IDD.

A recent study showed that higher mean T2 map values were found in the lower end plate zones than in upper end plate zones, both with unloading and axial loading, on MRI [36]. Consistent with the study, we found that T2 map values of the lower end plate, especially in the lower middle region, were higher than those of the upper end plate. Biomechanical studies indicate that the lower end plate, with a denser collagen network and less efficient transport properties, resists load more effectively than the upper end plate [37,38]. Moreover, the cartilaginous end

Supplementary Table 1
Correlation between the T1ρ and T2 map values of the nucleus pulposus (NP) and ROIs (the whole or front, middle, back one-third of the upper or lower end plate) in monkeys (A) or humans (B) had been analyzed by Pearson's correlation.

A.								
Monkey T1ρ Pearson r	NP vs. Upper mean	NP vs. UF	NP vs. UM	NP vs. UB	NP vs. lower mean	NP vs. LF	NP vs. LM	NP vs. LB
R	0.08038	0.1712	0.08953	0.2024	0.2179	0.1366	0.1554	0.2567
R square	0.006461	0.02931	0.008016	0.04095	0.0475	0.01865	0.02415	0.06592
P value	0.1912	0.0051	0.1453	0.0009	0.0003	0.0259	0.0112	<0.0001
P value summary	ns	**	ns	***	***	*	*	****
Significant? (a = 0.05)	No	Yes	No	Yes	Yes	Yes	Yes	Yes
Monkey T2 map Pearson r	NP vs. Upper mean	NP vs. UF	NP vs. UM	NP vs. UB	NP vs. lower mean	NP vs. LF	NP vs. LM	NP vs. LB
R	0.3341	0.1836	0.3838	0.08046	0.5597	0.2887	0.5334	0.2606
R square	0.1116	0.03369	0.1473	0.006474	0.3133	0.08333	0.2845	0.06791
P value	<0.0001	0.0074	<0.0001	0.2434	<0.0001	<0.0001	<0.0001	0.0001
P value summary	****	**	****	ns	****	****	****	***
Significant? (a = 0.05)	Yes	Yes	Yes	No	Yes	Yes	Yes	Yes
B.								
Human T1ρ Pearson r	NP vs. Upper mean	NP vs. UF	NP vs. UM	NP vs. UB	NP vs. Lower mean	NP vs. LF	NP vs. LM	NP vs. LB
R	0.2125	0.1743	0.304	−0.04205	0.1126	0.1836	0.05338	0.0234
R square	0.04515	0.03037	0.09243	0.001768	0.01268	0.03371	0.00285	0.0005478
P value	0.0973	0.1755	0.0163	0.7456	0.3835	0.1532	0.6803	0.8567
P value summary	ns	ns	*	ns	ns	ns	ns	ns
Significant? (a = 0.05)	No	No	Yes	No	No	No	No	No
Human T2 map Pearson r	NP vs. Upper mean	NP vs. UF	NP vs. UM	NP vs. UB	NP vs. Lower mean	NP vs. LF	NP vs. LM	NP vs. LB
R	0.4461	0.426	0.4721	0.2989	0.4574	0.3123	0.5636	0.2507
R square	0.199	0.1815	0.2229	0.08936	0.2092	0.09755	0.3176	0.06285
P value	0.0003	0.0006	0.0001	0.0183	0.0002	0.0135	<0.0001	0.0494
P value summary	***	***	***	*	***	*	****	*
Significant? (a = 0.05)	Yes	Yes	Yes	Yes	Yes	Yes	Yes	Yes

NP = nucleus pulposus; ROI = region of interest; LB = lower back; LF = lower front; LM = lower middle; UB = upper back; UF = upper front; UM = upper middle. *p<0.05, **p<0.01, ***p<0.001, ****p<0.0001

plate thickness decreases towards the centre of the disc and is associated with disc degeneration [39,40]. Taken together, these studies suggest that the upper end plate is less tolerant to age-related degeneration than the lower end plate and could explain our findings that degeneration of the lower end plate, especially the lower middle region, is closely associated with disc degeneration with age. However, sclerosis of the upper end plate may be associated with discogenic pain, causing LBP without IDD, because end plate sclerosis is accompanied by sensory nerve growth into porous end plates [41].

There are many animal models of IDD [42,43], but they do not mimic human disease very well. As humanoid primates, rhesus monkeys make a more physiologically relevant model than other animals for studying human IDD and LBP because of their anatomical similarities (e.g., walking and body size) [44,45]. In our previous study, we established a slowly progressing IDD model in rhesus monkeys by blocking nutrition exchange, which mimics the onset of disc degeneration in humans [17]. However, in the present study, we observed that the most common degenerative segment was mainly in the thoracolumbar (T12–T13) region of rhesus monkeys, which is different from the lower lumbar (L4–L5) region of human participants [46]. The discrepancy may be caused by the long-term arching for monkeys rather than bending for humans. These findings not only give a hint for future studies involving monkey models of IDD but also indicate that mechanical alteration of intervertebral discs caused by different postures and spinal curvature may also be important factors for IDD.

There are three limitations in the present study. First, the number of histology samples from rhesus monkeys was small, despite the number of monkeys enrolled in the study was considerable. However, there were different degenerative segments with different degrees of degeneration because each rhesus monkey had multiple intervertebral discs (T13–L7). Moreover, rhesus monkeys are very precious, and we sacrificed only one rhesus monkey in both the young and aged groups to minimize sacrificing nonhuman primates. Second, the number of human participants enrolled is small owing to the strict selection criteria to exclude participants with obvious disc herniation and vertebral instability. Although the data from human participants were consistent with the findings from rhesus monkeys, more clinical data are needed to support the results of the study. Third, this study is based on a single midsagittal 2D slice of the MRI image, which may lose some spatial information. Three-dimensional MRI scanning parameters will overcome this defect, which may be of benefit to find the changes of lateral end plate regions during ageing.

Conclusion

In conclusion, these data suggest that end plate degeneration can be quantitatively and precisely evaluated by T2 map in clinics. Furthermore, lower cartilage end plate degeneration was associated with disc degeneration during ageing, which indicates that T2 map may be used to evaluate end plate degeneration in the clinic.

Funding source

This work was supported by research grants from Beijing Municipal Health Commission (grant no. BMHC-2019-9); National Natural Science Foundation of Guangdong Province-Major Fundamental Research Fostering Program, China (2017A030308004); Key Project of NSFC-Guangdong Joint Program (U1601220, U0732001); and Science and Technology Program of Guangzhou (201704030082).

Author contributions

Xu.Z. and Z.L. conceived and designed the experiments; Z.L. and L.L. performed magnetic resonance imaging (MRI) for animals, data

acquisition, and data analysis. Q.Q. and Z.Z. performed histomorphometry staining. Y.C. and H.H. recruited outpatients at the clinic. Xi.Z. and D.L. performed MRI for participants. Z.L., L.L., and Xu.Z. drafted the manuscript. J.W., J.L., and X.C. contributed to data analysis and corrected the manuscript. All of the authors read and approved the final manuscript.

Conflict of Interest

The authors have no conflicts of interest to disclose in relation to this article.

Acknowledgements

The authors thank Qingqiang Tu at Small Animal Molecular Imaging Center, Laboratories of Translational Medicine and Clinical Research, Sun Yat-sen University, for facilitating microcomputed tomography and analysis.

References

[1] Manchikanti L. Epidemiology of low back pain. Pain Physician 2000;3:167–92.
[2] Katz JN. Lumbar disc disorders and low-back pain: socioeconomic factors and consequences. J Bone Joint Surg Am 2006;88(Suppl 2):21–4.
[3] Luoma K, Riihimaki H, Luukkonen R, Raininko R, Viikari-Juntura E, Lamminen A. Low back pain in relation to lumbar disc degeneration. Spine (Phila Pa 1976) 2000; 25:487–92.
[4] Livshits G, Popham M, Malkin I, Sambrook PN, Macgregor AJ, Spector T, et al. Lumbar disc degeneration and genetic factors are the main risk factors for low back pain in women: the UK Twin Spine Study. Ann Rheum Dis 2011;70:1740–5.
[5] Battie MC, Videman T, Levalahti E, Gill K, Kaprio J. Genetic and environmental effects on disc degeneration by phenotype and spinal level: a multivariate twin study. Spine (Phila Pa 1976) 2008;33:2801–8.
[6] Miller JA, Schmatz C, Schultz AB. Lumbar disc degeneration: correlation with age, sex, and spine level in 600 autopsy specimens. Spine (Phila Pa 1976) 1988;13: 173–8.
[7] Powell MC, Wilson M, Szypryt P, Symonds EM, Worthington BS. Prevalence of lumbar disc degeneration observed by magnetic resonance in symptomless women. Lancet 1986;2:1366–7.
[8] Battie MC, Videman T, Gill K, Moneta GB, Nyman R, Kaprio J, et al. 1991 Volvo Award in clinical sciences. Smoking and lumbar intervertebral disc degeneration: an MRI study of identical twins. Spine (Phila Pa 1976) 1991;16:1015–21.
[9] Videman T, Sarna S, Battie MC, Koskinen S, Gill K, Paananen H, et al. The long-term effects of physical loading and exercise lifestyles on back-related symptoms, disability, and spinal pathology among men. Spine (Phila Pa 1976) 1995;20: 699–709.
[10] Gullbrand SE, Peterson J, Ahlborn J, Mastropolo R, Fricker A, Roberts TT, et al. ISSLS prize winner: dynamic loading-induced convective transport enhances intervertebral disc nutrition. Spine (Phila Pa 1976) 2015;40:1158–64.
[11] Arpinar VE, Rand SD, Klein AP, Maiman DJ, Muftuler LT. Changes in perfusion and diffusion in the endplate regions of degenerating intervertebral discs: a DCE-MRI study. Eur Spine J 2015;24:2458–67.
[12] Herrero CF, Garcia SB, Garcia LV, Aparecido Defino HL. Endplates changes related to age and vertebral segment. BioMed Res Int 2014;2014:545017.
[13] Roberts S, Menage J, Urban JP. Biochemical and structural properties of the cartilage end-plate and its relation to the intervertebral disc. Spine (Phila Pa 1976) 1989;14:166–74.
[14] Urban JP, Holm S, Maroudas A, Nachemson A. Nutrition of the intervertebral disk. An in vivo study of solute transport. Clin Orthop Relat Res 1977:101–14.
[15] Gruber HE, Ashraf N, Kilburn J, Williams C, Norton HJ, Gordon BE, et al. Vertebral endplate architecture and vascularization: application of micro-computerized tomography, a vascular tracer, and immunocytochemistry in analyses of disc degeneration in the aging sand rat. Spine (Phila Pa 1976) 2005;30:2593–600.
[16] Gruber HE, Gordon B, Williams C, Norton HJ, Hanley Jr EN. Vertebral endplate and disc changes in the aging sand rat lumbar spine: cross-sectional analyses of a large male and female population. Spine (Phila Pa 1976) 2007;32:2529–36.
[17] Wei F, Zhong R, Wang L, Zhou Z, Pan X, Cui S, et al. Pingyangmycin-induced in vivo lumbar disc degeneration model of rhesus monkeys. Spine (Phila Pa 1976) 2015;40: E199–210.
[18] Roberts S, Johnson WE. Analysis of aging and degeneration of the human intervertebral disc. Spine (Phila Pa 1976) 1999;24:500–1.
[19] Farshad-Amacker NA, Farshad M, Winklehner A, Andreisek G. MR imaging of degenerative disc disease. Eur J Radiol 2015;84:1768–76.
[20] Mwale F, Iatridis JC, Antoniou J. Quantitative MRI as a diagnostic tool of intervertebral disc matrix composition and integrity. Eur Spine J 2008;17(Suppl 4): 432–40.
[21] Rauscher I, Stahl R, Cheng J, Li X, Huber MB, Luke A, et al. Meniscal measurements of T1rho and T2 at MR imaging in healthy subjects and patients with osteoarthritis. Radiology 2008;249:591–600.
[22] Stahl R, Luke A, Li X, Carballido-Gamio J, Ma CB, Majumdar S, et al. T1rho, T2 and focal knee cartilage abnormalities in physically active and sedentary healthy subjects versus early OA patients–a 3.0-Tesla MRI study. Eur Radiol 2009;19: 132–43.
[23] Duvvuri U, Reddy R, Patel SD, Kaufman JH, Kneeland JB, Leigh JS. T1rho-relaxation in articular cartilage: effects of enzymatic degradation. Magn Reson Med 1997;38:863–7.
[25] Pfirrmann CW, Metzdorf A, Zanetti M, Hodler J, Boos N. Magnetic resonance classification of lumbar intervertebral disc degeneration. Spine (Phila Pa 1976) 2001;26:1873–8.
[26] Duncan AE, Colman RJ, Kramer PA. Sex differences in spinal osteoarthritis in humans and rhesus monkeys (Macaca mulatta). Spine (Phila Pa 1976) 2012;37: 915–22.
[27] Zhou Z, Jiang B, Zhou Z, Pan X, Sun H, Huang B, et al. Intervertebral disk degeneration: T1rho MR imaging of human and animal models. Radiology 2013; 268:492–500.
[28] Pandit P, Talbott JF, Pedoia V, Dillon W, Majumdar S. T1rho and T2 -based characterization of regional variations in intervertebral discs to detect early degenerative changes. J Orthop Res 2016;34:1373–81.
[29] Johannessen W, Auerbach JD, Wheaton AJ, Kurji A, Borthakur A, Reddy R, et al. Assessment of human disc degeneration and proteoglycan content using T1rho-weighted magnetic resonance imaging. Spine (Phila Pa 1976) 2006;31:1253–7.
[30] Marinelli NL, Haughton VM, Munoz A, Anderson PA. T2 relaxation times of intervertebral disc tissue correlated with water content and proteoglycan content. Spine (Phila Pa 1976) 2009;34:520–4.
[31] Timmins PA, Wall JC. Bone water. Calcif Tissue Res 1977;23:1–5.
[32] Techawiboonwong A, Song HK, Wehrli FW. In vivo MRI of submillisecond T(2) species with two-dimensional and three-dimensional radial sequences and applications to the measurement of cortical bone water. NMR Biomed 2008;21: 59–70.
[33] Rad HS, Lam SC, Magland JF, Ong H, Li C, Song HK, et al. Quantifying cortical bone water in vivo by three-dimensional ultra-short echo-time MRI. NMR Biomed 2011; 24:855–64.
[34] Zhao J, Li X, Bolbos RI, Link TM, Majumdar S. Longitudinal assessment of bone marrow edema-like lesions and cartilage degeneration in osteoarthritis using 3 T MR T1rho quantification. Skeletal Radiol 2010;39:523–31.
[35] Gong J, Pedoia V, Facchetti L, Link TM, Ma CB, Li X. Bone marrow edema-like lesions (BMELs) are associated with higher T1rho and T2 values of cartilage in anterior cruciate ligament (ACL)-reconstructed knees: a longitudinal study. Quant Imag Med Surg 2016;6:661–70.
[36] Hebelka H, Miron A, Kasperska I, Brisby H, Lagerstrand K. Axial loading during MRI induces significant T2 value changes in vertebral endplates-a feasibility study on patients with low back pain. J Orthop Surg Res 2018;13:18.
[37] Grant JP, Oxland TR, Dvorak MF. Mapping the structural properties of the lumbosacral vertebral endplates. Spine (Phila Pa 1976) 2001;26:889–96.
[38] Gullbrand SE, Peterson J, Mastropolo R, Roberts TT, Lawrence JP, Glennon JC, et al. Low rate loading-induced convection enhances net transport into the intervertebral disc in vivo. Spine J 2015;15:1028–33.
[39] Moon SM, Yoder JH, Wright AC, Smith LJ, Vresilovic EJ, Elliott DM. Evaluation of intervertebral disc cartilaginous endplate structure using magnetic resonance imaging. Eur Spine J 2013;22:1820–8.
[40] Berg-Johansen B, Han M, Fields AJ, Liebenberg EC, Lim BJ, Larson PE, et al. Cartilage endplate thickness variation measured by ultrashort echo-time MRI is associated with adjacent disc degeneration. Spine (Phila Pa 1976) 2018;43: E592–600.
[41] Fields AJ, Liebenberg EC, Lotz JC. Innervation of pathologies in the lumbar vertebral end plate and intervertebral disc. Spine J 2014;14:513–21.
[42] Bian Q, Liang QQ, Wan C, Hou W, Li CG, Zhao YJ, et al. Prolonged upright posture induces calcified hypertrophy in the cartilage end plate in rat lumbar spine. Spine (Phila Pa 1976) 2011;36:2011–20.
[43] Kobayashi S, Baba H, Takeno K, Miyazaki T, Uchida K, Kokubo Y, et al. Fine structure of cartilage canal and vascular buds in the rabbit vertebral endplate. Laboratory investigation. J Neurosurg Spine 2008;9:96–103.
[44] Liang QQ, Cui XJ, Xi ZJ, Bian Q, Hou W, Zhao YJ, et al. Prolonged upright posture induces degenerative changes in intervertebral discs of rat cervical spine. Spine (Phila Pa 1976) 2011;36:E14–9.
[45] Bailey JF, Fields AJ, Liebenberg E, Mattison JA, Lotz JC, Kramer PA. Comparison of vertebral and intervertebral disc lesions in aging humans and rhesus monkeys. Osteoarthritis Cartilage 2014;22:980–5.
[46] Teraguchi M, Yoshimura N, Hashizume H, Muraki S, Yamada H, Minamide A, et al. Prevalence and distribution of intervertebral disc degeneration over the entire spine in a population-based cohort: the Wakayama Spine Study. Osteoarthritis Cartilage 2014;22:104–10.
[47] Michael T Modic, Thomas J Masaryk, Jeffrey S Ross, John R Carter. Imaging of degenerative disk disease. Radiology 1988;168:177–86. https://doi.org/10.1148/radiology.168.1.3289089.